Досліджено процес гомогенізації порошку діоксиду цирконію при вакуумно-дуговому виготовленні реакторних сталей. Процес гомогенізації запропоновано здійснювати в конвективному осередку з неплоским профілем дна і змішаними межами, який формується при переплаві сталі, з застосуванням катоду з поперечним перерізом типу «hollow fish-bone». Аналізується вплив форми катоду, розміру легуючих частинок, масопереносу в конвективному осередку на рівномірність розподілу діоксиду цирконію в розплаві сталі

Ключові слова: реакторна сталь, порошок оксиду, порожнистий катод, вакуумно-дуговий переплав, конвективний осередок, змішані граничні умови, масоперенос, гомогенізація

Исследован процесс гомогенизации порошка диоксида циркония при вакуумно-дуговом изготовлении реакторных сталей. Процесс гомогенизации предложено осуществлять в конвективной ячейке с неплоским профилем дна и смешанными пределами, который формируется при переплаве стали, с применением катода с поперечным сечением типа «hollow fish-bone». Анализируется влияние формы катода, размера легирующих частиц, массопереноса в конвективной ячейке на равномерность распределения диоксида циркония в расплаве стали

Ключевые слова: реакторная сталь, порошок оксида, полый катод, вакуумно-дуговой переплав, конвективная ячейка, смешанные граничные условия, массоперенос, гомогенизация

UDC 621.384.6:620.198
DOI: 10.15587/1729-4061.2016.79527

INVESTIGATION OF THE OXIDE PHASE CONVECTIVE HOMOGENIZATION WHILE VACUUM-ARC WITH HOLLOW CATHODE REMELTING OF STEEL

O. Andreeva
Postgraduate student***
Junior researcher
National Science Center
"Kharkiv Institute of Physics and Technology"
Akademicheskaya str., 1, Kharkiv, Ukraine, 61108
E-mail: andreevaoksana@kipt.kharkov.ua
B. Borts
Doctor of technical Science, Senior Researcher*
E-mail: borts@kipt.kharkov.ua
A. Kostikov
Doctor of Technical Sciences,
Associate Professor, Leading Researcher***
Professor
Department of Thermal Physics and Molecular Physics**
E-mail: kostikov@ipmach.kharkov.ua
V. Tkachenko
Doctor of Physics and Mathematics, Professor, Director*
Head of Department
Department of Physics of Innovative Energy & Technology & Ecology**
E-mail: tkachenko@kipt.kharkov.ua
*Sci. & Production Establishment
"Accelerating nuclear systems" of NSC "Kharkov Institute for Physics & Technology" of NAS of Ukraine
Akademicheskaya str., 1, Kharkiv, Ukraine, 61108
**V. N. Karazin Kharkiv National University
Svobody sq., 6, Kharkiv, Ukraine, 61022
***A. M. Pidgorny Institute for Mechanical Engineering Problems of of National Academy of Sciences of Ukraine
Pozharskogo str., 2/10, Kharkiv, Ukraine, 61046

1. Introduction

A lot of studies are being carried out recently to create construction materials which can be used for nuclear reactors of new generation, that are designed to work with higher temperatures and neutron flows within a reactor core (compared with currently existing reactors). Such materials should have high radiation and thermal resistance and low activation for fusion applications.

One of the ways to solve this task is to design and manufacture construction materials based on Oxide Dispersion Strengthened (ODS) steel.

ODS steel has nanometer sized oxide particles in it, which, for example, can be enriched with yttrium, oxygen, manganese, chrome or silicon. Such nanodispersed particles play an important part in raising of structural behavior and radiative properties of different materials [1, 2].

However, nowadays methods and proportions of ingoing material alloying with nanodispersed particles are studied not well enough, optimal mechanisms and temperatures of powders agglomeration still haven't been revealed. And these are just half of the issues as for ODS steels manufacturing technologies. The other half is about studies of attainability of high radiation resistance, heat

stability and low activation when utilization of produced materials.

That's why system study of the matters mentioned above seems to be rather challenging when designing and producing extra-strong alloys to be used in nuclear and thermonuclear power generation industry.

2. Literature review and problem statement

ODS steels due to their comparatively high stress-rupture properties, corrosion and radiation resistance are considered to be the most suitable ones for production of construction materials, which are planned to be used in improved nuclear reactors including the 4th generation reactors and DEMO nuclear reactor.

Such construction materials should resist the impact of high temperatures, enhanced neutron radiation flows and severe corrosion mediums the parameters and characteristics of which are far beyond the experience we've obtained while utilization of currently functioning nuclear power plants (NPP).

As for their quantitative and qualitative concepts, these materials should meet the following requirements [3]:

– low steel creep and dimensional stability at temperatures up to 970 K, durability about 9 years;

– high radiation resistance – up to radiation dose level of 250 DPA (number of displacements per atom) of neutron radiation;

– provide radiation resistance of the containment shell construction material at high thermal integrity characteristics;

– exhibit high mechanical properties: high rupture strength >300 MPa at 970 K, high-temperature stress-rupture strength >120 MPa for 10^4 hours at 970 K, total extension >1 %;

– exhibit high corrosion resistance to core coolants at high temperatures and such material should have high chemical compatibility while contacting with fuel material and sodium flow.

All examples mentioned below can serve as specific illustrations of ODS steels usage in the nuclear power generation industry:

– primary circuit tubes of integral fast reactors with gas and sodium coolants;

– nuclear fuel elements' shells in systems with sodium or supercritical water coolants.

Current ODS steel production uses metal powder industry [4] or hot isostatic pressing [5, 6] technologies.

The samples obtained by means of these technologies were studied by the method of small-angle neutron scattering, transmission electronic microscopy, atom-probe tomography, electron probe micro-analysis, diffraction as well as by mechanical tests conduction. The results of these studies had shown well-defined grain size distribution bimodality, which leads to metal ductility increase [8].

Study of properties of ODS steels ductility was performed for 9Cr-ODS steel with equal nominal content produced by means of hot isostatic pressing (HIP, steel was named COS-1) and spark plasma sintering (SPS, steel was named COS-2) [9]. The results had shown bimodal grain size distribution in COS-2 and more uniform grain size distribution in COS-1 steel samples, which indicates that COS-2 steel samples had higher metal ductility. Along with COS-2 steel samples ductility growth, nanooxides can also efficiently trap helium atoms and lead to formation of high-density ultrafine helium bubbles.

ODS ferrite/martensitic steel is high-tension steel at high temperatures, in the first place due to pinning of dislocations by oxide nanometer-sized particles. In reference [10] interaction between oxide particles and dislocations in 9Cr ODS ferrite steel was studied in different modes (static and dynamic one). There it was shown that the difference between the predicted and measured tensile strength level was due to spiral dislocations cross gliding on the oxide particles.

In reference [11 systematic studies of (H or He) blending atmosphere influence on the microstructure and mechanical properties of obtained alloys when producing of ODS steel with nominal content Fe–14Cr–0.3Y_2O_3 (wt. %) were conducted. The steel samples were manufactured using metal powder industry technology which includes mechanical alloying, hot isostatic pressing, forging and thermal treatment. It was shown that both blending atmospheres aided uniform distribution of Y-enriched nanoparticles within the final alloys. However, blending within H atmosphere leads to lower uniformity which in its turn decreases ductility characteristics of such ODS steels.

In reference [12] mechanically alloyed W-Ti ODS alloys made using metal powder industry technology were studied. Such alloys nowadays are considered to be rather promising materials for plasma components in progressive nuclear-power systems, since these materials have enhanced radiative and thermal properties. The results of these studies show that by spark plasma sintering it's possible to obtain a uniform fine-grained structure without forming a large number of Ti oxides which influence hardness and resilience modulus of W-Ti ODS alloys. It's suggested that microstructure homogeneity and mechanic properties of alloys can be additionally improved at the account of dispersoid oxide number increase.

In reference [13] mechanisms of Y, Ti, O solubilization within the ferrite matrix with further nanocluster deposition during the process of ODS steels mechanical alloying were studied. It was indicated that such ODS steels are promising materials for production of nuclear fuel elements for 4th generation nuclear reactors, since thick distribution of nanooxides within ODS steel provides good steel creep and radiation resistance.

The main issue when producing ODS steels by the methods mentioned above is that their manufacturing process is un-efficient (labor-consuming and expensive) when using metal powder industry technology as well as further power-consuming processing to bring the steel to its final state. One of the ways to resolve this issue is to create some new methods of ODS steel obtaining.

First of all, as one of such ways of ODS steel production, we should consider the method of vacuum-arc remelting of cylindrical steel blank, when in uniformly spaced apertures of its volume a certain mass of alloying agents of metal oxides nanodispersed powder is placed [14, 15].

This method is used to obtain 08X18H10T steel – nanostructured zirconium oxide dispersion strengthened steel. In [16] it was offered to use convective mass transfer in a cylindrical cell to describe the process of zirconium dioxide particles distribution along the liquid-alloy volume, that appears in a crystallizer pan. The influence of melting mode on zirconium oxide distribution parameters in ODS steel was studied theoretically and experimentally. It was

shown that reduction of zirconium oxide particles size leads to their more uniform distribution along the liquid-alloy volume.

In reference [17] the possibility of ODS steel production by using the vacuum-arc melting method upon 08X18H10T steel alloyed with zirconium oxide powder was analyzed. However, it was suggested to perform alloying by using some specially designed cathode shape (with "fish-bone" type cross profile). The influence of cathode shape and alloy agent particles size on uniform inflow of zirconium oxide into the steel liquid-alloy steel was studied theoretically.

Unlike reference [14], here it was suggested to describe zirconium oxide particles homogenization in the steel liquid-alloy basing on mass transfer in a cylindrical convection cell with non-flat bottom profile and free boundary conditions. It was shown that when using special cathode shape and small zirconium oxide particles it's possible to perform their uniform distribution within the liquid-alloy volume.

However, the results obtained in reference [17] don't allow us to describe homogenization of zirconium oxide powder in the liquid-alloy in case of its small initial mass fraction towards the cathode mass. Reduction of initial mass fraction of zirconium oxide may lead to the change of boundary condition type from free to solid or mixed one [18]. Under solid boundary conditions, the speed of mass transfer won't change significantly, but the rate of heat transfer decreases by 5.5 times, which may lead to liquid-alloy crystallization time increase. Therefore, not without interest is a theoretical analysis of zirconium oxide homogenization conditions when obtaining ODS steel 08X18H10T in a cylindrical convection cell with non-flat bottom profile and mixed boundary conditions.

3. Purpose and objectives of the study

This current study is aimed at analytical research of oxide phase homogenization processes by means of convection mass transfer in a cylindrical convection cell which appears in a crystallization pot during vacuum-arc remelting of stainless steel.

To achieve this aim it's necessary to solve the following tasks:

– describe the design of vacuum-arc-refining furnace cathode that would provide a uniform inflow of ZrO_2 powder into the liquid-alloy;

– calculate spatial distribution of liquid metal mass transfer convectional rate in a cylindrical cell with non-flat bottom profile and mixed boundary conditions;

– define ZrO_2 powder particles size which lets us observe their spatial homogenization;

– to describe melting and convectional homogenization process of ZrO_2 nanoparticles when vacuum-arc manufacturing of ODS steel.

4. Description of experimental unit for vacuum-arc remelting of steel alloyed with oxides micro- or nano-powder

In [7] the algorithm of ODS steel obtaining by means of consumable-electrode arc melting with nano- or microdisperse ZrO_2 powder uniformly distributed in it was described. There, crystallization pot in the form of cylindrical copper glass of 0.06 m in diameter was used as the anode. On the outside, this crystallization pot was cooled with flowing water. Steel cylindrical cathode with diameter. $D = 2R_0 = 0.03$ m and height $H = 0.20....0.25$ m was centered in the crystallization pot by means of special device that allows the cathode to move along the crystallization pot axis. The cathode has some cylindrical apertures with diameter 0.003–0.005 m and length less than the cathode radius, these apertures are drilled perpendicularly to its axis and uniformly along its azimuth and length, they are fully filled with micro- or nanodispersed ZrO_2 particles.

The apertures are closed tightly with thin plugs made of the same steel. Electric arc is fired and arching is sustained between the anode and cathode. Arching is kept by means of slow shifting of cathode upwards along the crystallization pot axis. Steel liquid-alloy flowing along the cathode surface absorbs ZrO_2 particles and forms a drop on the cathode lower brow, which is held on for some period of time by surface tension forces.

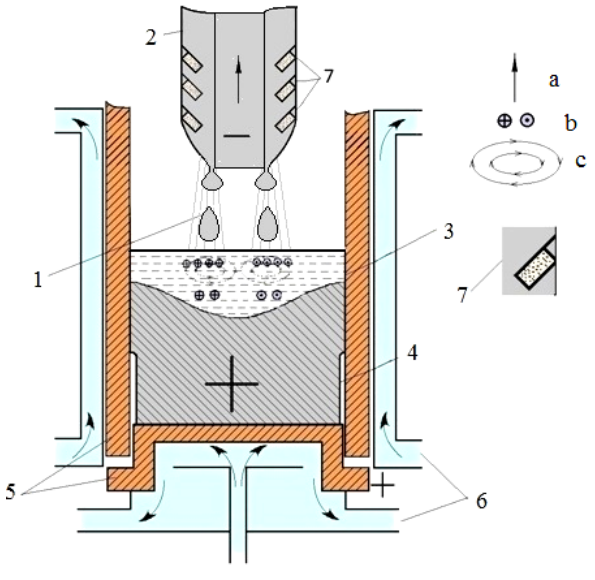

Fig. 1. Liquid-alloy flow when remelting of steel bar in vacuum-arc-refining furnace: *a* — electric current direction; *b* — metal circulation in horizontal plane; *c* — metal flow in vertical plane; 1 — corona; 2 — electrode that is being melt (cathode); 3 — liquid metal; 4 — steel bar; 5 — copper crystallizer pot (anode); 6 — coolant (water); 7 —apertures with alloying agent

When the drop mass increases it leads to its separation and fall into the crystallization pot, where a horizontal cylindrical liquid layer of molten metal is formed with ZrO_2 micro- or nano-particles distributed in it. Remelting is performed under the pressure about 10^3 Pa. Water cooled internal surfaces of crystallization pot enable fast liquid-alloy crystallization within 20–30 minutes.

5. Description of the cathode design

In reference [18] to increase the uniformity of zirconium dioxide powder inflow into the liquid-alloy it was suggested to use some specially designed cylindrical cathode with a "fish-bone" shaped cross section. At such a configu-

ration of the cathode, the drops of cathode molten together with ZrO_2 powder fall into the liquid layer of molten metal into the convection cell center where its upward stream can be observed. As a result, some percentage of zirconium dioxide is captured by a circulating metal flow and those particles that weren't captured get stuck on the crystallization pot walls. Thus, we can observe a decrease of zirconium dioxide content in ODS steel compared with its calculated value.

To prevent the ingress of drops of molten cathode with the ZrO_2 powder into the center of convection cell it is suggested to use hollow cathode (cylindrical cathode with hollow axial center not less than 10 mm), the algorithm of its usage is shown in Fig. 1.

Hollow cathodes are used, for example, in consumable electrode arc furnace in electrometallurgy for heating, melting, vacuum refining and alloying of ferrous and non-ferrous metals, for melting slag and flux metal, as well as mixing their liquid-alloys in mixers, ladle furnaces and complex steel processing facilities [19]. Arc and power supply parameters control is performed by pulsation overlapping upon total arc current and by supplying of plasma-supporting gas pulsating flow or alloying agents into the inter-electrode space through a hollow axial aperture in the cathode. Usage of such a cathode provides intensive and full mixing of the whole volume as well as on the molten pool surface, it decreases bottom electrodes thermal charge and at the same time increases their reliability and durability.

In the current study to insure better homogenization and the fullest utilization of dioxide powder in ODS steel production, unlike steel cathode scheme of "fish-bone" type that was described earlier in [17], here it was suggested to use hollow cathode shape, axial section of which forms a structure of "hollow fish-bone" type (Fig. 2).

According to the scheme shown in Fig. 2, some inclined circular grooves with Δx width are made on the surface of sleeve steel cathode 1, generating line of these grooves and the cathode radius form an angle equal to the natural slope of zirconium dioxide j (Fig. 2). Such grooves can be made, for example, by means of washer kit set 2 of a special shape and made from the same metal that the sleeve cathode is, which are then tightly pressed-on upon the latter. The cathode ready for a vacuum-arc remelting has a height equal to H = 0.20....0.25 m. Slope angle α of circular grooves axis against the cathode radius is defined experimentally. In our case, it was chosen to be significantly less than the natural slope of zirconium dioxide j so it would insure no powder spilling at the cathode vibration during remelting.

To prevent zirconium dioxide powder from spilling out from the cathode grooves during its movement when it is being installed into a vacuum chamber, all the system "hollow fish-bone" is being pressed-on into the thin-walled cylindrical tube 3 made from the same steel grade R_{123}.

The cathode design described in Fig. 2 insures uniform inflow of oxide powder into the liquid-alloy volume for all the time of vacuum-arc remelting. To describe parameters of the cathode of "hollow fish-bone" type completely it's necessary to indicate its characteristics [18]: pour density of zirconium dioxide powder ρ_{ZrO2}=2.76 g/cm^3; its natural slope φ=38° slope angle of circular grooves axis against the cathode radius α=φ/10.

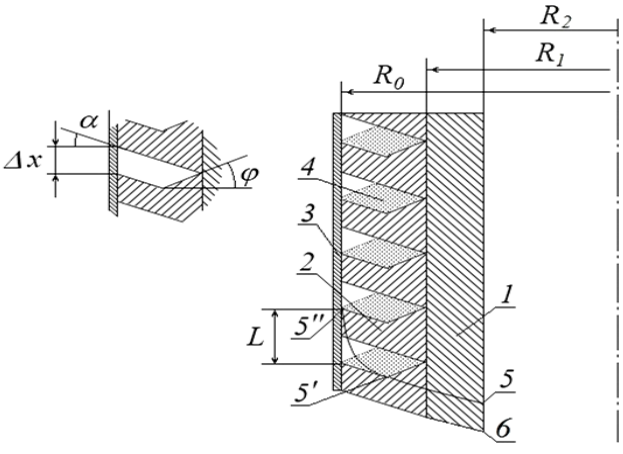

Fig. 2. Design of the cathode for vacuum-arc melting of ODS steel: 1 – sleeve cathode (outside radius R_1, internal one – R_2); 2 – specially shaped washer kit (outside radius R_0, internal one – R_1); 3 – thin-walled cylindrical tube; 4 – micro- or nanodispersed particles of ZrO_2; 5 – the cathode melting line; 5′ – point where ZrO_2 particles stop spilling out from the groove; 5″ – point where ZrO_2 particles start spilling out of the groove; 6 – the cathode lower brow, where the molten metal drops appear

6. Convection processes role in nanoparticles homogenization when obtaining ODS steel

The process of vacuum-arc remelting of steel alloyed with oxide nanopowders is analogous to the one described in [17], where oxide nanoparticles homogenization is performed due to heat and mass transfer of molten steel within a cylindrical convection cell with cosinusoidal bottom profile and free boundary conditions. These conditions appear in a convection cell in which the dispersed phase percentage is high enough. In the case studied in [17] it has to exceed 1.5 wt. %.

However, there are some situations when to alloy the steel it's necessary to add a small amount of dispersed phase, for example, less than 0.125 wt. %. In such a case solid boundary conditions appear on the cell bottom and mixed boundary conditions appear in a horizontal layer in general – on the upper boundary there are free boundary conditions and on the bottom one – solid boundary conditions.

Let's study below some fine dispersed ZrO_2 phase homogenization within molten stainless steel by means of convective mass transfer in a cylindrical convection cell with non-flat bottom profile and mixed boundary conditions.

7. Requirements that the cathode parameters should meet for vacuum-arc melting of ODS steel

To perform mixed boundary conditions it's necessary to add zirconium dioxide nanodispersed powder into the molten metal liquid-alloy in an amount not less than 0.125 wt. %. This requirement imposes some conditions upon the scheme of the cathode internal construction described in Fig. 2.

Zirconium dioxide powder mass M_{ZrO2}, located within the inclined circular groove is defined by the expression [18]:

$$M_{ZrO_2} = \pi R_0^2 \Delta x \rho_{ZrO_2} \left(1 - \frac{R_1^2}{R_0^2} - \frac{2R_1 \Delta x}{R_0^2 tg\varphi}\right). \quad (1)$$

When obtaining the expression (1) the condition $\varphi >> \alpha$, was taken into account as well as the condition of circular groove small width $\Delta x/R_0 << 1$.

We assume the time of inclined circular grooves forming on the cathode equal to L and their number equal to N – which is rather large, so the formula is valid LN=H, where N>>1. Hereafter, for all calculations let's assume N=10 for definiteness.

Let's consider steel blank mass to be equal to

$$M_{St} = \pi R_0^2 L \rho_{St},$$

where the time of inclined circular grooves forming is L, and $\rho_{St} = 7{,}27$ g/cm^3 – stainless steel density.

Thus, for mixed boundary conditions to be valid in elementary convection cell (ECC) this ratio should be true:

$$\frac{M_{ZrO_2}}{M_{St}} = \frac{N\Delta x \rho_{ZrO_2}}{H\rho_{St}} \left(1 - \frac{R_1^2}{R_0^2} - \frac{2R_1\Delta x}{R_0^2 tg\varphi}\right) \times$$
$$\times \left(\frac{R_0}{L}\frac{\Delta x}{R_0}\left(\frac{R_1}{R_0}\right)^2 - \left(\frac{R_2}{R_0}\right)^2\right)^{-1} =$$
$$= \gamma X \left(1 - Z^2 - \frac{2X \cdot Z}{tg\varphi}\right)\left(\delta^{-1} X Z_1^2 - Z_2^2\right)^{-1} \le 0.125 \cdot 10^{-2}, \quad (2)$$

where

$$X = \frac{\Delta x}{R_0}, \quad \gamma = \frac{1}{\delta} \cdot \frac{\rho_{ZrO_2}}{\rho_{St}}, \quad \delta = \frac{L}{R_0}, \quad Z_1 = \frac{R_1}{R_0}, \quad Z_2 = \frac{R_2}{R_0}.$$

We should mention that in (2) the inequality $XZ_1^2 > \delta Z_2^2$ should also be fulfilled.

Continuous inflow of zirconium dioxide powder into the liquid-alloy volume is performed at the condition when points 5″ and 5′ are located on the cathode melting line shown in Fig. 2. To get this condition, we assume the cathode melting line 5 to be given as $z = \beta_{St} r^d$, where z and r are vertical and horizontal coordinates of the cathode points correspondingly, $\beta_{St} = \beta / R_0^{d-1}$ is a constant value for such metal, β and d are dimensionless constants defined experimentally.

To determine the value of power exponent d the set of experiments was performed to study the process of cylindrical water icicle melting (9 cm in diameter and 17 cm high). Digital processing of the icicle frontal images while it was melting provided us with the power value that varies within a range d=2.63...3.96. For the further calculations let's assume the power value to be equal to 3.

Based on the above stated, the condition of zirconium dioxide powder uniform inflow into the liquid-alloy volume can be written as follows:

$$\frac{H}{NL} = \frac{H/NR_0\beta}{\left(1 - \left(\frac{R_1}{R_0}\right)^3 - \frac{3\Delta x}{R_0 tg\varphi} \cdot \left(\frac{R_1}{R_0}\right)^2\right)} = \frac{\delta/\beta}{\left(1 - Z_1^3 - \frac{3Z_1^2 X}{tg\varphi}\right)} = 1. \quad (3)$$

Unlike it was done in [8], let's consider the cathode diameter to be equal to $D_0=2R_0=4$ cm and its height H=20 cm when performing numerical calculations. Cathode aperture diameter is assumed to be equal to $D_2=2R_2=1$ cm.

At such parameters simultaneous solution of the inequality (2) on the upper boundary and the equation (3) for the following values of parameters, that meet the experiment requirements β=15, γ=0.38, δ=1 gives us the following value of nondimensional width of inclined circular groove and internal radius of a washer kit ratio against cylindrical cathode radius X=0.19 and Z_1=0.783 correspondingly. Reduction of zirconium dioxide content to be less than 0.125 wt. % actually doesn't change the value of the groove width and the washer kit internal radius value mentioned above.

Thus, in this section, it was demonstrated that by a specific selection of the hollow cathode parameters and by taking into account physical properties of nanodispersed ZrO_2 powder, it's possible to insure mixed boundary conditions on the bottom of cylindrical convection cell as well as uniform inflow of the powder into the molten liquid-alloy volume.

8. The structure of ECC with cosinusoidal bottom profile

To describe the structure of ECC with non-flat bottom profile let's consider a cylindrical convection cell placed in the layer of viscous incompressible liquid which is infinite along the x and y axes with thickness h where the lower boundary of the cell is described by rotational surface with generatric line:

$$z = -\left(\cos\left(\pi r R_c^{-1}\right) + 1\right)\Delta h/2, \quad (4)$$

which has an axis common with a cylindrical cell. Here R_c is an elementary cylindrical convection cell radius, Δh – the biggest deviation of the cell non-flat lower boundary. Axis z is directed upwards and perpendicularly to the layer boundaries z=0 and z=h (Fig. 3).

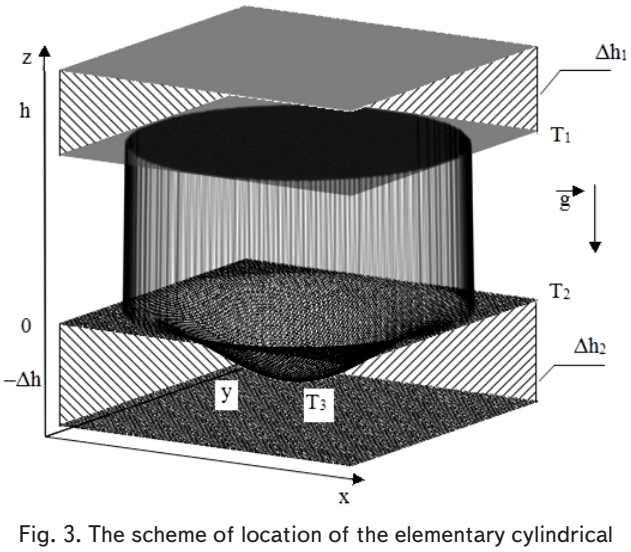

Fig. 3. The scheme of location of the elementary cylindrical convection cell with radius R_c in the layer of viscous incompressible liquid with thickness h and cosinusoidal bottom profile

Temperature distribution along the layer thickness $T_0(z)$ is assumed to be a linear function of the coordinate z. The temperature of the cell lower boundary is higher than the

one of the upper boundary: $T_0(0)=T_2$, $T_0(h)=T_1$ $(T_2>T_1)$, and temperature of the boundary lowest point is equal to

$$T_0(-\Delta h)\equiv T_3=T_2+\Delta T_{bot}\left(\Delta T_{bot}>0\right).$$

In the absence of disturbances the linear dependence of temperature on coordinate z gives us the following values of its gradients:

$$\vec{\nabla}T_0(z)=-\frac{\Theta}{h}\vec{e}_z\left(0\le z\le h\right),$$

$$\vec{\nabla}T_0(z)=-\frac{\Delta T_{cone}}{\Delta h}\vec{e}_z\left(-\Delta h\le z\le 0\right), \qquad (5)$$

where $\Theta=T_2-T_1$ is temperature differential between the lower and upper planes, $\vec{e}_z$ – unit vector directed along the axis z, $\Delta T_{bot}=\Theta\Delta h/h$.

9. Spatial distribution of convective mass transfer within ECC with cosinusoidal bottom profile

Stokes lines $\psi_{1,2}(r,z)$ of the cylindrical cell with non-flat bottom profile and free boundary conditions, according to the Fujiwhara effect and analogically to the problem studied in [8] for ECC with conical bottom profile will be defined by a superposition of Stokes functions of two vortices placed one above another. The upper one depicts the vortex in a cylindrical cell with flat free boundaries, the second and the lower one depicts the vortex in a cylindrical cell with non-flat bottom profile and mixed boundary conditions:

$$\psi_{1,2}(r,z)=A_0\left(1-\vartheta_{1,2}\left(z\frac{1+\Delta h}{\Delta h},r\right)\right)\psi_0(r,z\Delta h), \qquad (6)$$

where

$$\psi_0(r,z)=r\frac{R_c}{\sigma_{1,1}}\sin\left(\frac{\pi}{\Delta h}z\right)J_1\left(\frac{\sigma_{1,1}}{R_c}r\right),$$

where $\sigma_{1,1}$ – the first zero of the Bessel function of the first order and the 1st kind,

$$\vartheta_1(r,z)=J_0\left(\sigma_{0.1}\left(z/\Delta h-\left(\cos(\pi r/R_c)-1\right)/2\right)\right)$$

and

$$\vartheta_2(r,z)=\cos\left(\left(z/\Delta h-\left(\cos(\pi r/R_c)-1\right)/2\right)\pi/2\right)$$

is model functions that insure solid boundary conditions within the cell with cosinusoidal bottom profile.

In Fig. 4, *b* as a result of the Fujiwhara effect application (overlapping of two vortices within a cell) Stokes lines are depicted for an elementary cylindrical convection cell with cosinusoidally deepened bottom profile and with mixed boundary conditions. Maximal depth of cosinusoidal cell bottom is equal to $\Delta h=1/3$.

The calculation shows that for the model functions $\vartheta_1(r,z)$ and $\vartheta_2(r,z)$ Stokes lines in the united cells look like concentric smooth closed lines, the shape of which reflects the curved cosinusoidal bottom profile. Such a shape of Stokes lines (as it was indicated for conical bottom profile [8]) also indicates the formation of convective flow in the form of one vortex within a cell with mixed boundary conditions.

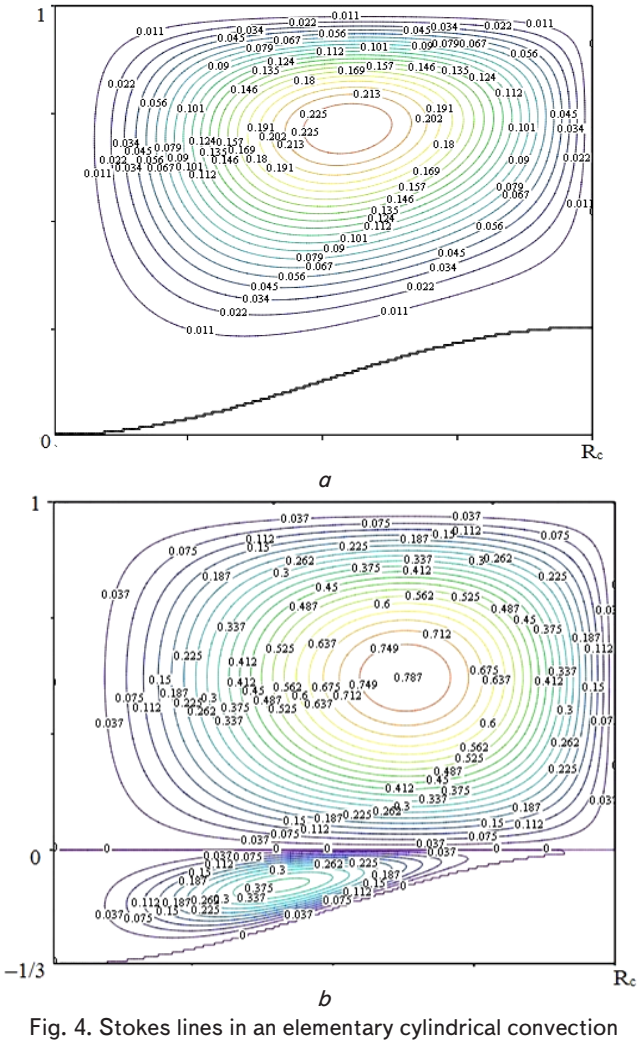

Fig. 4. Stokes lines in an elementary cylindrical convection cell with mixed boundary conditions with cosinusoidally deepened bottom profile with its maximum depth $\Delta h=1/3$ for a model function $\vartheta_1(r, z)$: *a* – before the cells union; *b* – after the cells union

10. ZrO_2 particles size and their homogenization condition in ODS steel volume

Let's study the process of ODS steel melting through the example of convective mixing of ZrO_2 nano- or micro-dispersed inclusions within the liquid-alloy volume of stainless steel 08X18H10T.

To analyze ZrO_2 particles homogenization in the volume of ODS steel, let's assume the following conditions to be valid [7]:

1. Nanoparticles don't dissolve in the stainless steel, but they form suspended solid particles which means that iron oxide surface film is formed on their surface;

2. Boundary conditions on a convection cell bottom are solid ones [11], since liquid steel with addition of less than 0.125 wt. % of ZrO_2 powder nanoparticles doesn't form a new phase towards the pure metal liquid-alloy, i. e. the induced velocity and normal derivative of vertical velocity are equal to zero.

Horizontal and vertical velocity of mass transfer in ECC with non-flat bottom profile in the absence of ZrO_2 nanoparticles can be defined using Stokes functions (6):

$$v_{r,1,2}(r,z) = -\frac{1}{r}\frac{\partial \psi_{1,2}(r,z)}{\partial z}, \quad v_{z,1,2}(r,z) = \frac{1}{r}\frac{\partial \psi_{1,2}(r,z)}{\partial r}. \qquad (7)$$

Also, as well as in the case studied in [7], addition of micro- and nanoparticles of ZrO_2 into the molten metal will lead to multidirectional forces action on these particles: upward Archimedes force (always upward directed); gravity force (always directed downwards); frictional force (Stokes force) (directed along the vector of convective liquid motion). The resultant force of all these forces at sufficiently small size of zirconium dioxide nanoparticles can support them in the liquid-alloy for quite a long time and then lead to homogenization. For that to happen the molten metal drops have to inflow into the liquid-alloy close to the convection cell axis around Stokes lines area with the amplitudes from 0.046 to 0.162. In this case, similar to the numerical calculations given in [7–9], convective flows capture zirconium dioxide particles and distribute them within the cell volume and at the same time they simultaneously homogenize them.

11. Criteria of convective homogenization of ZrO_2 particles

In vacuum-arc-refining furnace, the cathode material made from metal drops contacting ZrO_2 nanoparticles is accumulated on the circular generating line of the cathode aperture lower part and it falls on the surface of the cylindrical convection cell according to the same circular generating line that the cathode has.

Metal drops will penetrate at least at a distance of 0.5 mm from the cell axis. Here, zirconium dioxide nanoparticles surmount gravity and go upwards due to Archimedes and Stokes forces action. Close to the cell upper boundary small amount of nanoparticles is being carried away by a radial flow to the crystallization pan wall and settles there. Another amount of the particles goes to the cell bottom under the action of gravity and Stokes force which exceed the value of Archimedes force. These particles get into the closed convective flow and they are exposed to convective mixing inside the ECC, which in its turn is equivalent to their uniform distribution within the ODS steel sample volume.

Criterion of Archimedes force surmount (homogenization condition) applies the following restriction upon the particles size [7, 9]:

$$r_p \le 10^{-2}\sqrt{v_c \frac{9\nu}{2g}\frac{\Delta l}{R_c}\frac{\rho_l}{\rho_l - \rho_p}} \ \text{(m)}, \qquad (8)$$

where $v_c \approx 1...3$ cm/sec – is experimentally measured maximum velocity of molten metal transfer along the cell upper horizontal surface; ν – kinematic viscosity of liquid metal; g – free fall acceleration; Δl – average distance between micro- and nanoparticles; R_c – radius of cylindrical convection cell; ρ_1, ρ_p – liquid metal and zirconium dioxide density correspondingly.

Under the experiment conditions, all nano- or micro-particles of ZrO_2 together with the drop-shaped molten cathode metal in the upper left corner of the cell (Fig. 5) will penetrate into the cell volume. Then the particles that got into the liquid metal of the cell will move along the flow line inside the cell (lines II) or to the crystallization pan wall (lines I).

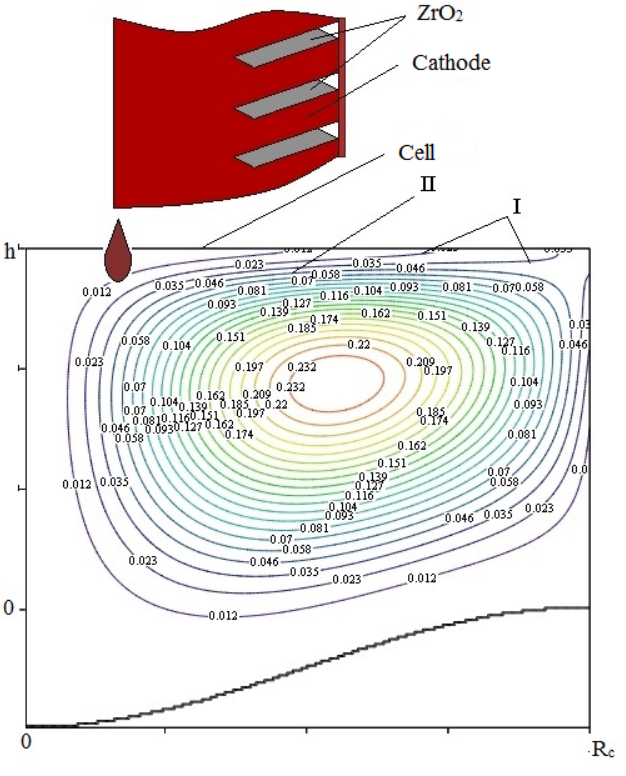

Fig. 5. The scheme of ZrO_2 particles transfer within the convection cell. The digitized lines correspond to the flow lines

In the experimental conditions the inequality (8) demonstrates that ZrO_2 particles which size is $r_p < 90$ nm will be distributed uniformity along the ODS steel bar and the particles which size exceeds 160 nm have to be taken to the crystallization pan wall by the convection flow.

On the assumption of the above mentioned the following conclusions may be stated:

– drops of the cathode metal will penetrate into the cylindrical convection cell along the circular line which corresponds to the inner circle of the hollow cathode;

– penetration of cathode material drops to a depth corresponding to the cell half-height insures uniform distribution of ZrO_2 particles within the cell volume;

– ZrO_2 particles that are less than 90 nm large should be uniformly distributed within the sample volume.

12. Conclusions

1. It was suggested to use a specially designed hollow cathode to improve the uniformity of zirconium dioxide powder inflow into the liquid-alloy in vacuum-arc-refining furnace. Such a construction of the hollow cathode allows to insure mixed boundary conditions in a cylindrical convection cell and it enables uniform inflow of ZrO_2 nanodispersed powder into the molten metal volume.

2. Spatial distribution of convective mass transfer velocity of liquid metal within a cylindrical cell with cosinusoidal bottom profile was described. It was shown that flow lines

(Stokes lines) in a convection cell are concentric smooth closed lines, the shape of which reflects the distorted cosinusoidal bottom profile. Such a shape of the flow lines indicates the formation of convective flow in the form of one vortex within a cell with mixed boundary conditions.

3. Horizontal and vertical velocities of mass transfer in ECC with non-flat bottom profile in the absence of ZrO_2 nanoparticles are defined by the Stokes function. At sufficiently small size of zirconium dioxide particles it's possible to surmount Archimedes upward force acting on a particle due to gravity and Stokes friction forces, which in its turn enables the particles homogenization. To do so the drops of the cathode molten metal have to inflow into the liquid-alloy close to the convection cell axis within the area of Stokes lines with amplitudes from 0.046 to 0.162.

4. The criteria of convectional homogenization of ZrO_2 nanoparticles were stated. These criteria are as follows:

– cathode material drops penetrate into the cylindrical convection cell along the circular line which corresponds to the inner circle of the hollow cathode;

– cathode material drops penetrate to a convection cell depth corresponding to the cell half-height;

– ZrO_2 particles that are less than 90 nm large will stay in the liquid-alloy for quite a long time and then homogenize in the liquid-alloy volume as a result of convective mass transfer.

References

1. Rogozhkin S. V. Atom probe characterization of nano-scaled features in irradiated ODS Eurofer steel [Text] / S. V. Rogozhkin, A. A. Aleev, A. G. Zaluzhnyi, A. A. Nikitin, N. A. Iskandarov, P. Vladimirov et. al. // Journal of Nuclear Materials. – 2011. – Vol. 409, Issue 2. – P. 94–99. doi: 10.1016/j.jnucmat.2010.09.021
2. Rogozhkin, S. V. Atom probe study of radiation induced precipitates in Eurofer97 Ferritic-Martensitic steel irradiated in BOR-60 reactor [Text] / S. V. Rogozhkin, A. A. Nikitin, A. A. Aleev, A. B. Germanov, A. G. Zaluzhnyi // Inorganic Materials: Applied Research. – 2013. – Vol. 4, Issue 2. – P. 112–118. doi: 10.1134/s2075113313020160
3. Azarenkov N. A. Nanostructural Materials in the Nuclear Engineering [Text] / N. A. Azarenkov, V. N. Vojevodin, V. G. Kirichenko, G. P. Kovtun, V. V. Kurinny, S. V. Lytovchenko // The Journal of KNU. Physical series «Nuclei, Particles, Fields». – 2013. – Vol. 1059, Issue 2/58. – P. 19–29.
4. Antsyferov, N. Poroshkovaia metallurhyia y napilenyia pokrityia [Text] / N. Antsyferov, H. V. Bobrov, L. K. Druzhynyn et. al. – Moscow: Metallurhyia, 1987. – 792 p.
5. Aheev, V. S. Yspolzovanye metodov metallurhyy raspilennikh y bistrozakalennikh poroshkov dlia yzghotovlenyia obolochek tvelov yz dyspersno-uprochnennikh oksydamy (DUO) zharoprochnikh ferrytno-martensytnikh stalei [Text] / V. S. Aheev, A. A. Nykytyna, V. V. Saharad, B. V. Safronov, A. P. Chukanov, V. V. Tsvelev // VANT. Seryia: Fyzyka radyatsyonnikh povrezhdenyi y radyatsyonnoe materyalovedenye. – 2007. – Vol. I, Issue 2. – P. 134–141.
6. Aheev, V. S. Horiachee yzostatycheskoe pressovane metallycheskykh poroshkov [Text] / V. S. Aheev, V. L. Hyrshov // Komplekt: YTO. – 2015. – Vol. 08. – P. 28–30.
7. Hilger, I. Fabrication and characterization of oxide dispersion strengthened (ODS) 14Cr steels consolidated by means of hot isostatic pressing, hot extrusion and spark plasma sintering [Text] / I. Hilger, X. Boulnat, J. Hoffmann, C. Testani, F. Bergner, Y. De Carlan et. al. // Journal of Nuclear Materials. – 2016. – Vol. 472. – P. 206–214. doi: 10.1016/j.jnucmat.2015.09.036
8. Pozdniakov, V. A. Plastychnost nanokrystallycheskykh materyalov s bymodalnoi zerennoi strukturoi [Text] / V. A. Pozdniakov // Pysma v ZhTF. – 2007. – Vol. 33, Issue 23. – P. 36–42.
9. Lu, C. Microstructure of HIPed and SPSed 9Cr-ODS steel and its effect on helium bubble formation [Text] / C. Lu, Z. Lu, R. Xie, C. Liu, L. Wang // Journal of Nuclear Materials. – 2016. – Vol. 474. – P. 65–75. doi: 10.1016/j.jnucmat.2016.03.010
10. Ijiri Y. Oxide particle–dislocation interaction in 9Cr-ODS steel [Text] / Y. Ijiri, N. Oono, S. Ukai, S. Ohtsuka, T. Kaito, Y. Matsukawa // Nuclear Materials and Energy. – 2016. doi: 10.1016/j.nme.2016.06.014
11. Auger, M. A. Effect of the milling atmosphere on the microstructure and mechanical properties of a ODS Fe-14Cr model alloy [Text] / M. A. Auger, V. de Castro, T. Leguey, S. Lozano-Perez, P. A. J. Bagot, M. P. Moody, S. G. Roberts // Materials Science and Engineering: A. – 2016. – Vol. 671. – P. 264–274. doi: 10.1016/j.msea.2016.06.054
12. Chen, C.-L. Effect of consolidation and oxide dispersoid addition on phase formation and mechanical properties of W-Ti ODS alloy [Text] / C.-L. Chen, Y. Zeng // International Journal of Refractory Metals and Hard Materials. – 2016. – Vol. 60. – P. 11–16. doi: 10.1016/j.ijrmhm.2016.06.012
13. Loyer-Prost, M. High resolution transmission electron microscopy characterization of a milled oxide dispersion strengthened steel powder [Text] / M. Loyer-Prost, J.-S. Merot, J. Ribis, Y. Le Bouar, L. Chaffron, F. Legendre // Journal of Nuclear Materials. – 2016. – Vol. 479. – P. 76–84. doi: 10.1016/j.jnucmat.2016.06.050
14. Borts, B. V. Yssledovanye vozmozhnosty poluchenyia dyspersno-uprochnennikh oksydamy (DUO) stalei metodom vakuumno-duhovoho pereplava [Text] / B. V. Borts, A. F. Vanzha, Y. M. Korotkova, V. Y. Sityn, V. Y. Tkachenko // VANT. Seryia: Fyzyka radyatsyonnikh povrezhdenyi y radyatsyonnoe materyalovedenye. – 2014. – Vol. 4, Issue 92. – P. 117–124.
15. Bozbiei, L. S. Investigation of the Oxide Phase Homogenization in the Convective Cell While Producing Vacuum–Arc Remelting [Text] / L. S. Bozbiei, B. V. Borts, I. M. Neklyudov, V. I. Tkachenko // Eastern-European Journal of Enterprise Technologies. – 2016. – Vol. 2, Issue 5 (80). – P. 14–21. doi: 10.15587/1729-4061.2016.65424
16. Patochkina, O. L. Elementary Convection Cell in the Horizontal Layer of Viscous Incompressible Liquid with Rigid and Mixed Boundary Conditions [Text] / O. L. Patochkina, B. V. Borts, V. I. Tkachenko // East-European J. of Phys. – 2015. – Vol. 2, Issue 1. – P. 23–31.
17. Patent RU 2293268, MPK F27V3/08. Sposob elektroplavky v duhovoi pechy postoiannoho toka [Text] / Yachykov Y. M., Morozov A. P., Portnova Y. V. – 2005115622/02, declareted: 23.05.2005, published: 10.02.2007, Bul. 4, 10.
18. Gershuni, G. Z. Convective stability of incompressible fluid [Text] / G. Z. Gershuni, E. M. Zhuxovickij. – Moscow: Nauka, 1972. – 393 p.